## PAPER

Check for updates

# Phytocat – a bio-derived Ni catalyst for rapid de-polymerization of polystyrene using a synergistic approach†

Parul Johar, [a] Elizabeth L. Rylott, [b] C. Robert McElroy, [a] Avtar S. Matharu [a] and James H. Clark [*a]

Environmentally-friendly recycling of polystyrene and disposal of metal-containing plant biomass from phytoremediation sites are major challenges. Strategies beyond waste-to-energy that can harness the circular chemical potential of such feed-stocks are needed. We present a "triple-green" approach using microwave irradiation (250 °C, 200 W, <10 min) for the accelerated de-polymerization of polystyrene and valorization of nickel-contaminated biomass to yield valuable chemical building blocks. Biomass from soil-grown *Stackhousia tryonii* plants that naturally hyperaccumulate nickel (1.5 wt%), alongside non-hyperaccumulator, hydroponically-grown willow (*Salix viminalis*, 0.1 wt% Ni) was tested. The presence of naturally-bound nickel in carbonized biomass (Ni-phytocat) from *S. tryonii* and *S. viminalis* was shown to significantly accelerate de-polymerization (74% and 69% styrene selectivity; 18 kJ g$^{-1}$ and 24 kJ g$^{-1}$ microwave energy consumed, respectively) when compared to control *S. viminalis* (<0.01 wt% Ni; 56%; 42 kJ g$^{-1}$) and activated carbon (57%; 36 kJ g$^{-1}$). The Ni-phytocat offered significant advantage in enabling rapid de-polymerization of polystyrene with up to 91% conversion efficiency as compared to control phytocat (up to 82%) and activated carbon (up to 79%) within 5 min. Use of this synergistic effect of bio-derived Ni and microwaves to maximize the de-polymerization efficiency is proposed.

## Introduction

The production of plastics is an energy intensive process, accounting for 62–108 MJ kg$^{-1}$ of feed-stock energy.[1] Around 4% of fossil-fuel extracted annually (natural gas liquid fraction or low-value gaseous fraction from petroleum refining) is presently used as a raw material for plastics.[1] By 2050, the global production of plastics is expected to account for 20% of petroleum consumed globally and 15% of the annual carbon emissions.[1,2] Currently, less than 10% of the total plastic waste generated (>6300 Mt) is recycled, yet even if increased, this is not a long-term solution.[3] Furthermore, repeated recycling results in decreased mechanical quality, alongside issues of mixing of different plastic types and contamination with additives (plasticizers such as phthalate esters, flame retardants such as polybrominated diphenyl ethers and stabilizers such as phenolic anti-oxidants), which reduces product quality.[4,5]

Current recycling processes also add substantially to the energy burden of using plastics. New strategies are needed for the selective de-polymerization of plastics, either to their constituent monomers for recycling into virgin plastics, or as feed-stocks for other chemical processes.[4,5] To this end, the microbial degradation of hydrolysable plastics, for example, polyethylene terephthalate (PET), polycarbonate and polyurethane is more likely in the environment than for non-hydrolysable polymers (polystyrene (PS), polyethylene and polypropylene) that are predominantly found as pollutants in marine environment.[6] Functional groups, such as esters, carbonates, and urethanes, allow much faster degradation *via* hydrolysis than plastics without functional groups, such as PS, even though they contain tertiary C–H bonds.[7] Moreover, due to inadequate recycling, most of the polystyrene waste generated ends up in oceans.[8] Recent studies revealed that styrene oligomers (SOs) were leached from PS plastic weathering in marine environments even at low temperatures.[8,9] A large variation in global SOs concentration was observed (10–31 400 µg kg$^{-1}$), with a global average value of 3679 µg kg$^{-1}$ in coastal beach sand samples.[9]

Many possibilities exist to create a world where carbon emissions are minimized and valuable chemical resources are recycled using environmentally-friendly methods and applying

*aGreen Chemistry Centre of Excellence, Department of Chemistry, University of York, York, YO10 5DD, UK. E-mail: james.clark@york.ac.uk*
*bCentre for Novel Agricultural Products, Department of Biology, University of York, Wentworth Way, York, YO10 5DD, UK*
†Electronic supplementary information (ESI) available. See DOI: 10.1039/d0gc03808c

green chemistry principles.[10,11] Towards this goal is the use of renewable feed-stocks to generate advanced, carbon-based materials such as catalysts, *via* energy efficient, inexpensive methods.[12,13] A major feedstock is plant biomass from non-food crops such as willow (*Salix* spp. and hybrids) and *Miscanthus* hybrids.[14] In order to supply sufficient biomass, bio-refineries require increasing areas of land to be dedicated to these biomass crops, putting pressure on existing agricultural land use. A solution could be to grow biomass crops on polluted land unsuitable for food or feed focused agriculture. The estimated global area of contaminated land has the potential to produce approximately 10% of world total energy needs through biomass crops.[14] Major contaminants include heavy metals, among which is nickel (Ni).[15] Some soils contain naturally high levels of Ni, but significant contamination has also occurred from anthropogenic activities such as industrial land use (*e.g.* metallurgy and metal surface-treatment plants), mining and waste disposal. Estimates suggest that approximately 5% (8.75 Mha) of E.U. agricultural land area has Ni contamination above the ecological threshold.[16] Phytomining, the use of plants to extract metals, is now used commercially on Ni-rich, serpentine soils.[17] While Ni is a micronutrient essential for plant growth, at higher levels it is phytotoxic to many plant species. To overcome this phytotoxicity, the phytomining technology uses Ni-hyperaccumulator plants. These are species that have evolved to flourish on Ni-rich soils, taking up many fold higher levels of the metal from their surrounding environment into their tissues (up to 1000 mg kg$^{-1}$ dry tissue).[18]

Phytoremediation, the use of plants to remove or degrade pollutants from the environment, is increasingly used to restore previously contaminated land for agricultural production.[17] This technique offers numerous benefits, including being a relatively simple, often cost-effective solution that leads to a reduction in soil-and air borne pollution, as well as increased soil functionality and biodiversity.[17] However two major hurdles with this technology are (1) the development of biomass-producing plant lines with the ability to take up, and tolerate, significant levels of contaminating metals and (2) the effective recycling of the resulting metal-containing plant biomass. Towards the first hurdle is the use of *Salix* spp. and hybrids. Although *Salix* spp. are not hyperaccumulators, some species and hybrids in this genus have the ability to take up, and tolerate relatively high levels of Ni for non-hyperaccumulator species, and have been shown to grow well on Ni-contaminated soils.[18] Furthermore, some *Salix* spp. and hybrids are also able to tolerate other metals, often found as soil co-contaminants (As, Pb, Zn *etc.*).[18,19] The Salicaceae contain species with a genetically diverse range of phenotypes, and studies suggest that it is likely to include broad variation in the ability to withstand Ni tolerance, and rate of Ni uptake.[19] This variation offers the opportunity to use breeding to improve the desired Ni tolerance and uptake traits. Using willow has the advantages that it is a high biomass crop that grows vigorously in a broad range of environmental conditions and geographical locations, and is farmed using existing agricultural infrastructure.[17]

Towards the second hurdle, recovering Ni from the metal-containing non-hyperaccumulator biomass is not currently economical, and at present, the biomass is incinerated, the Ni recovered and the ash used in construction or land-filled.[20,21] Nickel-rich biomass can be used to produce a bio-catalyst, thereby potentially negating the use of virgin-mined metal for catalyst production.[22–25] Ni-based biocatalysts offer a huge variety of hybrid platforms consisting of naturally-occurring, inorganic components with lignocellulose providing an exciting opportunity to advance green chemistry applications.[25–27] Biomass conversion into bio-char using non-conventional, microwave pyrolysis, is more energy efficient than conventional techniques and allows the fine tuning of chemical structure and morphology.[28,29] Microwave pyrolysis is gaining attention at both pilot and industrial scale, as an efficient and economical process owing to the short processing time and uniform volumetric heating of the feedstock.[30,31] Recently Ni has been applied in pyrolysis-based experiments to improve tar reforming activity through its high efficiency in breaking C–C and C–H bonds.[27,31]

Microwave assisted co-pyrolysis of biomass with plastics is an emerging, sustainable approach for enhancing product value and process energy efficiency, with only a few reported studies.[32–37] Jakab *et al.* studied co-pyrolysis of PS with charcoal and lignocellulosic materials and reported that the char from lignocellulosic materials enhanced the hydrogenation of the PS monomer to increase the yields of hydrogenated aromatics, such as toluene and ethyl benzene.[38] Currently, there is much focus on developing new catalysts to promote the synergistic properties of biomass and plastics, and to enhance products composition and yields.[39–42] However, the use of synthetic catalysts in pyrolysis technology makes the overall process more energy intensive, economically expensive (*e.g.* through the use of scarce metals) and often less sustainable.[43–50]

The aim of this study is to achieve value-added recyclability of metal-containing plant biomass harvested from contaminated land remediation sites, alongside plastic waste by developing a Ni-phytocat for de-polymerization of polystyrene to valuable chemicals. Overall, this "triple-green" approach investigates the synergistic valorization of Ni contaminated biomass and PS waste streams using an energy efficient process as depicted in Fig. 1.

Our research demonstrates the microwave-assisted accelerated de-polymerization of PS, in the presence of Ni containing bio-char derived from Ni-rich willow (0.1 wt% Ni) and hyperaccumulator species, *S. tryonii* (1.5 wt% Ni). This was used to examine the impact of naturally-bound Ni in a plant matrix as a catalyst for de-polymerization, thereby avoiding the need for traditionally-mined metal. The control experiments were conducted using bio-char derived from willow grown in hydroponic medium that was not dosed with Ni (<0.01 wt% Ni) and activated carbon. To test the ability of our Ni-based biocatalyst (termed Ni-phytocat) to depolymerize PS, it was mixed with PS (1 : 1, 1 : 2, 1 : 5, 1 : 10 and 1 : 20 by weight) and pyrolyzed (MW: 250 °C, 200 W) to produce styrene enriched oil, together with low amounts of gas and char.
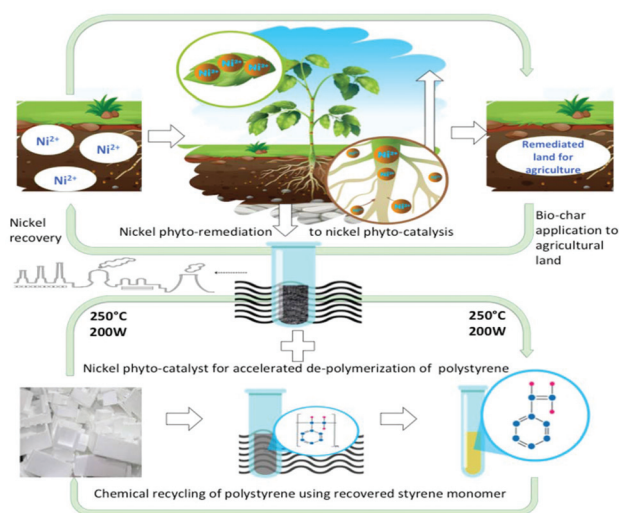
**Fig. 1** Schematic representation of the triple green approach to demonstrate the pathway of Ni-phyto-remediation to Ni-phyto-catalysis for accelerated de-polymerization of polystyrene.

# Results and discussion

### Pathway of Ni-phyto-accumulation to Ni-phyto-catalysis

Following dosing with 100 mg kg$^{-1}$ Ni for two weeks, the plants exhibited mild toxicity symptoms, notably the yellowing of younger leaves (see Fig. 2a–c).[49] Air-dried, ground, aerial tissues contained 0.05 wt% Ni. Bio-derived Ni catalyst was prepared by microwave-assisted pyrolysis (250 °C) of the tissues to produce *S. viminalis* bio-char (0.1 wt% Ni, termed Ni-phytocat-0.1), and a *S. tryonii* bio-char (1.5 wt% Ni, termed Ni-phytocat-1.5). The control catalyst was prepared using *S. viminalis* bio-char that had not been dosed with Ni (<0.01 wt% Ni, termed as control phytocat).

In Ni-rich biomass, Ni acts as an *in situ* catalyst during pyrolysis, improving the quality and value of the products.[50,51] Pyrolysis also reduces Ni toxicity as it favors char aromatization and stabilization of Ni in the matrix. Moreover, low temperature (250 °C) microwave-assisted pyrolysis requires less energy consumption and reduced time compared to other thermal processes.[51,52] Pyrolysis of raw, and Ni impregnated, willow biomass was investigated under different temperatures and showed that Ni could promote C–H and C–O bonds cleavage in the char, thereby reducing char yield.[32,52] Nickel must be in

the zero oxidation state (Ni$^0$) to produce a catalytic effect on biomass pyrolysis.[32,51] This active form can be produced by the pyrolysis of the Ni ion withing the willow, most likely Ni$^{2+}$, at temperatures below 500 °C,[48] and is consistent with our study including surface analysis and application of these phyto-catalysts for accelerated de-polymerization of PS.

### Understanding phytocat by its surface composition and morphology

Nickel forms complexes with various plant-based ligands (histidine, organic acids, nicotianamine and proteins) to facilitate uptake of Ni$^{2+}$ in plants as these ligands possess high association constant for Ni$^{2+}$ ions.[49] On pyrolysis, the Ni$^{2+}$ species are reduced by the carbon matrix to form the catalytically active Ni$^0$ in the phytocat.[50] A study using Ni impregnated willow wood pellets established that Ni remains in an active metal form during pyrolysis if some of the carbon is left in the system.[50,51] Using *in situ* X-ray photoelectron spectroscopy (XPS), we demonstrated that the low activity state is bulk NiO which is reduced to the active Ni$^0$ state. In particular, catalysts with low Ni content are dominated by Ni$^{2+}$ along with some sequestered Ni$^0$ sites.[52,53] The differences in Ni loading causes changes not only in its distribution but also in the surface chemistry and consequently the catalytic activity.[54] However, an oxide layer formed around supported Ni particles can suppress coke formation while preserving high catalytic activity.[52]

The surface composition and valence states of the characteristic elements in Ni-phyto-cat were determined by XPS. The high-resolution XPS scans of the C 1s, N 1s, O 1s and Ni 2p regions, including the curve-fitting spectra for phyto-cat containing 0.1 and 1.5 wt% Ni, are depicted in ESI Fig. 1.† The peak around 852 eV is assigned to Ni$^0$ and peaks between 855 and 861 eV are assigned to Ni$^{+2}$ in the form of NiO.[52] The surface of the phytocat consisted of both Ni$^0$ and NiO. As observed in ESI Fig. 1a,† with increasing Ni content, there is an increase in Ni$^0$ peak with a simultaneous decrease in Ni$^{+2}$ peak.

Deconvoluted high-resolution N 1s XPS spectra of phytocat display the peaks located at 398.8, 399.7, 400.7, and 402.3 eV (ESI Fig. 1b†) attributed to pyridinic N, pyrrolic N, graphitic N, and oxidized N, respectively.[53] The position of the pyrrolic N peak shifted to a higher value for the higher Ni loadings, which is probably due to charge transfer between Ni and pyrrolic N species.[53]

Deconvoluted high-resolution C 1s XPS spectra of phytocat show characteristics peaks for C–C (284.5 eV), C–N (285.3 eV), C–O (286.1 eV), C=O (287.1 eV), and O–C=O (288.8 eV) bonds.[52] The prominent peaks at 284.3–284.5 eV reveal that the most carbons in the phytocat are aromatic. The presence of these functional groups on the surface of phytocat facilitates its binding with Ni particles.

The O 1s spectra of phytocat catalysts (ESI Fig. 1d†) all comprised three peaks, among which the peaks at 529.9–530.9 eV corresponding to the lattice oxygen involved in the metal framework oxide (Ni–O) while the peaks at 531.6–532.8 eV are assigned to oxygen atoms bonded to carbon atoms (C=O
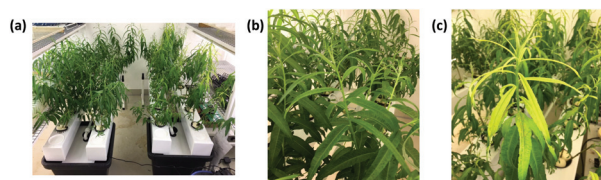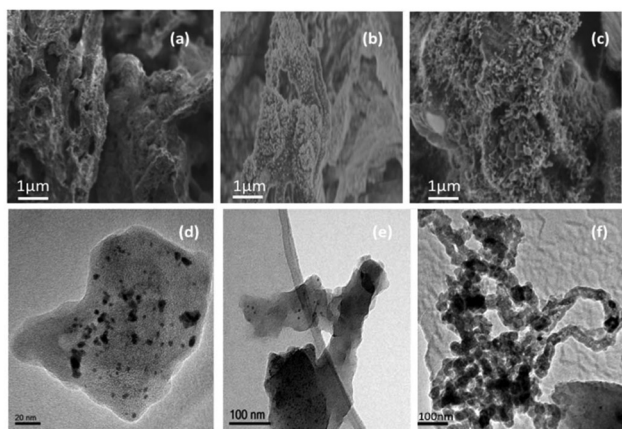


**Fig. 2** Aeroflo system (general hydroponics) (a) used to grow willow rods (*Salix viminalis*, 6 weeks duration) for preparation of phyto-catalyst using (b) no Ni dosing and (c) Ni dosing (100 mg kg$^{-1}$, 2 weeks duration).

**Fig. 3** Scanning electron migrograph (a: control phytocat, b and c: Ni phytocat) and Transmission electron micrographs (d and e: Ni phytocat and f: spent Ni phytocat).



**Fig. 4** Product distribution and composition on de-polymerization of polystyrene (PS) by microwave processing at 200 W and 250 °C using (a and b) Ni-phytocat-1.5, (c and d) Ni-phytocat-0.1, (e and f) control phytocat and (g and h) activated carbon using various mixing ratios with polystyrene (1 : 1, 1 : 2, 1 : 5, 1 : 10, 1 : 20 by weight).

bond), and the peaks at higher binding energy of 533.1–534.4 eV are attributed to the chemisorbed oxygen species from C–O in carbonates ($CO_3^{2-}$).[52,53]

The uniformity of pyrolyzed clusters of carbon increased with increasing Ni content in the carbon matrix as observed in the scanning electron micrographs (SEM; Fig. 3a–c). Unlike control phytocat (Fig. 3a), numerous outgrowths were observed in Ni-phytocat representing uniform carbon growth at the surface of bio-char (Fig. 3b and c). Transmission electron microscopy (TEM) micrographs showed that many small particles (representing Ni) emerged well-packed in the carbon matrix with increasing Ni content (0.1 wt%, Fig. 3d and 1.5 wt% Fig. 3e respectively). The TEM micrograph of the spent phytocat showed the formation of carbon fibers containing Ni in the matrix (Fig. 3f). There was an observed increase in the degree of graphitization in the spent phytocat. A direct correlation was found between the Ni particle size and the amount of carbon deposited.[50,51,53]

**Effect of nickel concentration in the phytocat on de-polymerization of polystyrene**

Both naturally-bound Ni (Ni-phytocat-1.5) and hydroponically-infused Ni (Ni-phytocat-0.1) play a significant role in the microwave assisted de-polymerization of PS (18 kJ g$^{-1}$ and only 24 kJ g$^{-1}$ of microwave energy is consumed to reach the set-point of 250 °C in less than 2 min, respectively) compared to the control phytocat (42 kJ g$^{-1}$ of microwave energy consumed and almost double the time to reach the set-point) and activated carbon (36 kJ g$^{-1}$ of microwave energy consumed and double the time to reach the set-point) (ESI Fig. 3a and b†). The Ni-phytocat-1.5 offered significant advantage in enabling rapid de-polymerization of PS (up to 91% conversion efficiency) as compared to Ni-phytocat-0.1 (up to 84%), control phytocat (up to 81%) and activated carbon (up to 79%) within 5 min (ESI Fig. 4†). This demonstrated the highly energy efficient mechanism of Ni-phytocat assisted PS de-polymerization under microwave irradiation. In general, the phytocat,
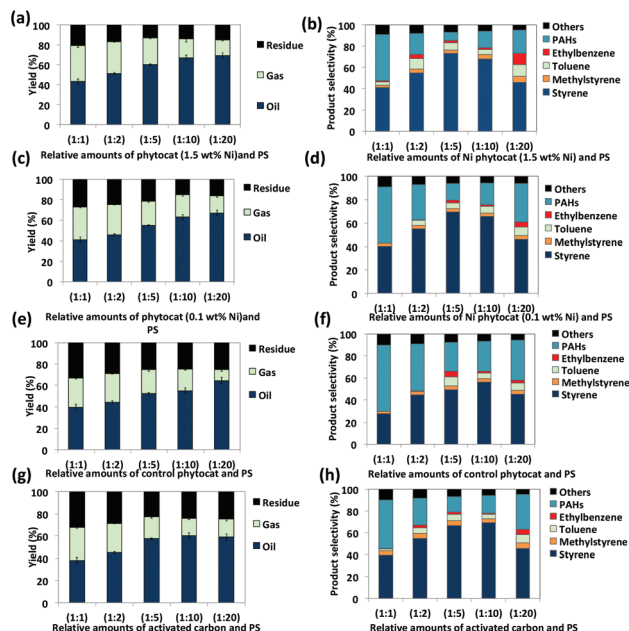
and activated carbon, aids in transfer of the microwave energy as heat energy to PS, achieving high heating rates. The addition of phytocat and activated carbon to PS significantly affected the product yield and composition (Fig. 4).

Oil (72.5%) and gas (21.4%) yields were higher using Ni phytocat-1.5 than Ni phytocat-0.1 (67% oil and 16.7% gas), control phytocat (64.5% oil and 15.9% gas) and activated carbon (61.0% oil and 14.4% gas), thereby showing the influence of Ni in promoting side cracking reactions.

Pyrolysis oils produced post microwave irradiation of PS were rich in aromatic hydrocarbons (styrene, α-methyl styrene, toluene and ethylbenzene as the major compounds) and consistent with the literature (Fig. 4b, d, f and h) and ESI† file.[54–57] Ni-phytocat-1.5 produced more monocyclic aromatics (85%) as compared to Ni-phytocat-0.1 (79.4%), control phytocat (66%) and activated carbon (79.1%). The highest selectivity for styrene was observed with Ni-phytocat-1.5 (up to 74%) as compared with Ni-phytocat-0.1 (up to 69.5%), control phytocat (up to 56%) and activated carbon (up to 57%). The increased yield of mono-aromatics originating from the primary radicals shows that more chain scissions occur, which requires a higher decomposition temperature whereas using our phytocat we were able to achieve this under much milder conditions (250 °C, <10 min) than normal (>400 °C, >10 min).[60,61]

**Effect of mixing ratio of catalyst and polystyrene**

The relative amounts of PS and catalyst significantly affected the de-polymerization efficiency. Using the phytocat materials,

the de-polymerization efficiency improved on increasing PS content up to 1 : 20 ratio (82–91% conversion efficiency). While with activated carbon, the maximum conversion efficiency was achieved at 1 : 5 ratio (77%) with a gradual decrease on increasing PS content to 1 : 20 ratio (ESI Fig. 4†). The peak reduction in time and energy consumed under microwave irradiation to reach the set-point of 250 °C was observed with a catalyst to PS ratio of 1 : 5 by weight, followed in order by 1 : 10, 1 : 1, 1 : 2 and 1 : 20 by weight.

The volume of pyrolysis gas produced reduced with increasing PS content. This is possibly due to an increased production of aromatic compounds with better thermal stability, leading to lower thermal cracking and thus lower gas yields (Fig. 4a, c, e and g).[43] Short residence time also favours the suppression of cracking reactions.[44] The char yield decreased with increasing PS content, with peak reduction observed using a 1 : 10 ratio with Ni-phytocat-1.5 (11.2%), Ni-phytocat-0.1 (14.1%) and control phytocat (21.4%) and activated carbon (22.2%) with a further slight increase at 1 : 20 ratio. The maximum total conversion (oil + gas yield) was achieved at 1 : 10 ratio with Ni-phytocat-1.5 (93.9%), Ni-phytocat-0.1 (84%) compared to the control phytocat (76%), while a 1 : 5 ratio was best for activated carbon (77.5%).

The production of ethyl benzene and toluene increased with increasing phytocat : PS ratios (with lowest at 1 : 1 and highest at 1 : 20, by weight) and can be attributed to increased production of styrene and its higher rate of hydrogenation due to the presence of catalytic Ni[0.39,58] Moreover, with increasing residence time, there is reduced production of styrene.[39] Similar observations were noted with the pyrolysis oil obtained from a 1 : 20 ratio where the styrene produced was reduced to around 47% (Ni-phytocat-1.5), 46.1% (Ni-phytocat-0.1), 45.4% (control phytocat) and 45.6% (activated carbon), while production of toluene and ethyl benzene increased to around 11% (Ni-phytocat-1.5), 7.2% (Ni-phytocat-0.1), 6.3% (control phytocat), 7.3% (activated carbon) and 10% (Ni-phytocat-1.5), 4.3% (Ni-phytocat 0.1), 2.5% (control phytocat), 4.8% (activated carbon) respectively. Hence the relative amounts of catalyst and PS dictates both efficiency and selectivity of the de-polymerization reaction.

### Comparison of conventional heating (TGA-FTIR) and microwave heating on quality of de-polymerization products

The functional groups of evolved gases were determined using simultaneous TGA/FT-IR analysis in real-time (Fig. 5a–c). Under a conventional set-up, de-polymerization of PS initiated once the temperature had reached approximately 425 °C. (ESI Fig. 8†). However, under microwave heating, the de-polymerization temperature in the presence of phytocat significantly decreased to below 250 °C and within 5 minutes of the reaction time. No such effect was observed in the absence on Ni-phytocat even after 30 minutes of reaction time at 200 W and 250 °C. This result proves the highly energy efficient mechanism of phytocat assisted de-polymerization using microwave processing.
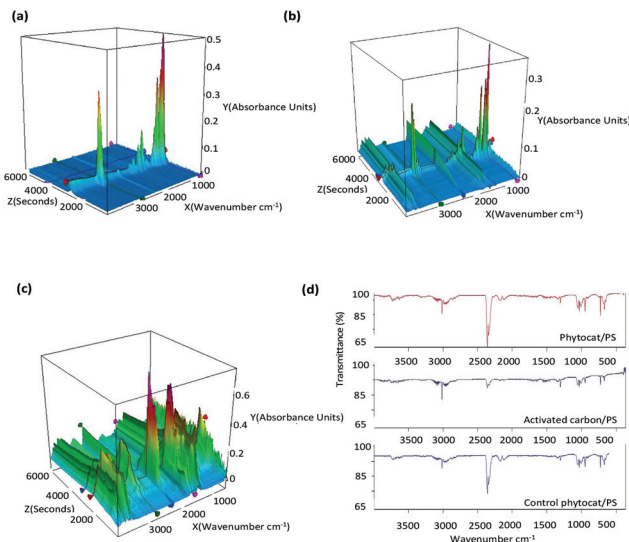


Fig. 5 Production and testing of phytocat using conventional pyrolysis set-up using TG-FTIR (a) Polystyrene (PS), (b) Ni-phytocat-1.5 and polystyrene mixture (1 : 1 by weight) (c) biomass containing Ni (1.5 wt%); evolved gas analysis after microwave processing (d) using IR spectroscopy.

During pyrolysis, short chain radicals are produced from C–C bond cleavage and reaction with PS.[60,61] De-polymerization of PS occurs, resulting in the production of styrene monomers, as shown from the changes in the Fourier-transform infrared (FTIR) fingerprint region occurring (1000 and 500 cm$^{-1}$). For the pyrolysis of plant biomass containing Ni (Fig. 5c), removal of carbonyl groups and decarboxylation reactions of carboxylic acid groups lead to evolution of $CO_2$ (as shown by asymmetrical stretching observed between 2250 and 2500 cm$^{-1}$ and bending vibrations between 580 and 730 cm$^{-1}$).[45] During the co-pyrolysis, 3-D spectra obtained by thermogravimetric analysis coupled with Fourier transform infrared (TG-FTIR, Fig. 5b) of phytocat and PS mixtures were obtained in order to investigate the interactions of radicals. There is an observed increase in production of $CH_4$ (3100–2800 cm$^{-1}$) and CO (2250–2000 cm$^{-1}$) due to interaction of phytocat and PS.

The gas produced during de-polymerization of PS using microwave irradiation was analyzed using FTIR for qualitative analysis (Fig. 5d). The evolved gas mainly consisted of $CO_2$, CO, $CH_4$, and $C_2H_4$ which suggests that the main reaction leading to the formation of gas is the de-alkylation of the styrene formed and de-alkylation of methyl-substituted bi- and tricyclic aromatic hydrocarbons.[62,63]

The results from published studies on the pyrolysis (<700 °C) of plastics were compared with our study (ESI Table 1†). In our study, a significant reduction in reaction time (<10 min) and temperature (250 °C) meant less energy consumption to valorize the plastic waste as compared with other studies. This is an important improvement if we are to develop industrial plastic waste based chemical production processes.

## Conclusions

Our study demonstrates the biosynthesis of catalytically active Ni in phytocat using microwaves, thereby avoiding the need for traditionally mined metal. The use of bio-derived Ni in phyto-cat was investigated for the synergistic valorization of PS to produce predominantly monocyclic aromatics (up to 85%).

The presence of naturally-bound Ni was shown to accelerate de-polymerization of PS (up to 74% styrene selectivity in an oil yield up to 72% %; 18 kJ $g^{-1}$ microwave energy consumed) using microwaves under much milder conditions (200 W, 250 °C, <10 min) than at which de-polymerization is normally conducted (>400 °C, >10 min).[59–64] The Ni-phytocat offered significant advantage in enabling rapid de-polymerization of PS with up to 91% conversion efficiency as compared to control phytocat (up to 82%) and activated carbon (up to 79%) within 5 min. Using the phytocat materials, the de-polymerization efficiency improved on increasing PS content up to a 1 : 20 ratio while the activated carbon was most effective up to 1 : 5 ratio, with a gradual decrease in efficiency with increasing PS content. This result shows the highly energy efficient mechanism of Ni-phytocat to de-polymerize PS, even at low metal concentrations. The technique created in this work could not only help solve the problem of heavy-metal-laden biomass waste produced from phyto-remediation of metal-contaminated land, but also expand the utilization of bio-char as an effective catalyst for the de-polymerization of environmentally problematic waste plastics. Overall, this "triple-green" approach was successful in synergistic valorization of Ni-containing biomass and plastic waste streams using an energy efficient process. Further optimization of the system is now required to develop this technology for industrial application.

## Conflicts of interest

There are no conflicts to declare.

## Acknowledgements

## References

1 L. Lebreton and A. Andrady, *Palgrave Commun.*, 2019, **5**, 1–11.
2 B. Gibb, *Nat. Chem.*, 2019, **11**, 394–395.
3 R. Geyer, J. Jambeck and K. Law, *Sci. Adv.*, 2017, **3**, 1700782.
4 Plasticseurope.org, 2020.
5 A. Turner and M. Filella, *Mar. Pollut. Bull.*, 2020, **158**, 111352.
6 M. Krueger, H. Harms and D. Schlosser, *Appl. Microbiol. Biotechnol.*, 2015, **99**, 8857–8874.
7 K. Min, J. Cuiffi and R. Mathers, *Nat. Commun.*, 2020, **11**, 1–11.
8 B. Gewert, M. Plassmann and M. MacLeod, *Environ. Sci.: Process. Impacts*, 2015, **17**, 1513–1521.
9 B. Kwon, K. Amamiya, H. Sato, S. Chung, Y. Kodera, S. Kim, E. Lee and K. Saido, *Chemosphere*, 2017, **180**, 500–505.
10 S. Davis, K. Caldeira and H. Matthews, *Science*, 2010, **329**, 1330–1333.
11 V. Scott, R. Haszeldine, S. Tett and A. Oschlies, *Nat. Clim. Change*, 2015, **5**, 419–423.
12 M. He, Y. Sun and B. Han, *ChemInform*, 2013, **44**, 11936–11950.
13 B. Cheng, B. Huang, R. Zhang, Y. Chen, S. Jiang, Y. Lu, X. Zhang, H. Jiang and H. Yu, *Sci. Adv.*, 2020, **6**, 0748.
14 J. E. Campbell, D. Lobell, R. Genova, A. Zumkehr and C. Field, *Environ. Res. Lett.*, 2013, **8**, 035012.
15 E. Ander, C. Johnson, M. Cave, B. Palumbo-Roe, C. Nathanail and R. Lark, *Sci. Total Environ.*, 2013, **454–455**, 604–618.
16 G. Tóth, T. Hermann, G. Szatmári and L. Pásztor, *Sci. Total Environ.*, 2016, **565**, 1054–1062.
17 K. Kennen and N. Kirkwood, *Phyto: principles and resources for site remediation and landscape design*, Routledge, 2015.
18 A. Tognacchini, T. Rosenkranz, A. Van der Ent, G. E. Machinet, G. Echevarria and M. Puschenreiter, *J. Environ. Manage.*, 2020, **254**, 109798.
19 C. F. Ng, H. Ye, L. She, H. Chen and S. Y. Lai, *Appl. Catal., A*, 1998, **171**(2), 293–299.
20 I. Y. Efimochkin, O. A. Bazyleva, E. G. Arginbayeva and A. N. Bolshakova, *Inorg. Mater. Appl. Res.*, 2020, **11**, 297–303.
21 A. J. Hunt, C. W. N. Anderson, N. Bruce, A. M. García, T. E. Graedel, M. Hodson, J. A. Meech, N. T. Nassar, H. L. Parker, E. L. Rylott, K. Sotiriou, Q. Zhang and J. H. Clark, *Green Process Synth.*, 2014, **3**(1), 3–22.
22 T. E. Graedel, R. Barr, C. Chandler, T. Chase, J. Choi, L. Christoffersen, E. Friedlander, C. Henly, C. Jun, N. T. Nassar and D. Schechner, *Environ. Sci. Technol.*, 2012, **46**(2), 1063–1070.
23 G. M. Mudd, *Ore Geol. Rev.*, 2010, **38**(1–2), 9–26.
24 T. Norgate and S. Jahanshahi, *Miner. Eng.*, 2011, **24**(7), 698–707.
25 D. S. Su, S. Perathoner and G. Centi, *Chem. Rev.*, 2013, **113**, 5782–5816.
26 C. R. Catlow, M. Davidson, C. Hardacre and G. J. Hutchings, *Philos. Trans.: Math., Phys. Eng. Sci.*, 2016, **374**(2061), 20150089.
27 Z. A. Harumain, H. L. Parker, A. Muñ oz Garcì a, M. J. Austin, C. R. McElroy, A. J. Hunt, J. H. Clark, A. J. Meech, C. W. Anderson, L. Ciacci and T. E. Graedel, *Environ. Sci. Technol.*, 2017, **51**(5), 2992–3000.
28 Y. Richardson, J. Motuzas, A. Julbe, G. Volle and J. Blin, *J. Phys. Chem. C*, 2013, **117**(45), 23812–23831.

29 C. Wu, V. L. Budarin, M. Wang, V. Sharifi, M. J. Gronnow, Y. Wu, Y. J. Swithenbank, J. H. Clark and P. T. Williams, *Appl. Energy*, 2015, **157**, 533–539.

30 H. Yang, R. Yan, H. Chen, D. H. Lee and C. Zheng, *Fuel*, 2007, **86**, 1781–1788.

31 Y. Zhang, H. Lei, Z. Yang, K. Qian and E. Villota, *ACS Sustainable Chem. Eng.*, 2018, **6**(4), 5349–5357.

32 M. Hu, M. Laghari, B. Cui, B. Xiao, B. Zhang and D. Guo, *Energy*, 2018, **145**, 228–237.

33 J. M. Melillo, J. M. Reilly, D. W. Kicklighter, A. C. Gurgel, T. W. Cronin, S. Paltsev and C. A. Schlosser, *Science*, 2009, **326**, 1397–1399.

34 M. Brebu, S. Ucar, C. Vasile and J. Yanik, *Fuel*, 2010, **89**, 1911–1918.

35 G. Özsin and A. E. Pütün, *J. Cleaner Prod.*, 2018, **205**, 1127–1138.

36 D. V. Suriapparao, B. Boruah, D. Raja and R. Vinu, *Fuel Process. Technol.*, 2018, **175**, 64–75.

37 B. B. Uzoejinwa, X. He, S. Wang, A. E. F. Abomohra, Y. Hu and Q. Wang, *Energy Convers. Manage.*, 2018, **163**, 468–492.

38 E. Jakab, M. Blazso and O. Faix, *J. Anal. Appl. Pyrolysis*, 2001, **58**, 49–62.

39 R. Prathiba, M. Shruthi and L. R. Miranda, *Waste Manage.*, 2018, **76**, 528–536.

40 X. Zhang, H. Lei, S. Chen and J. Wu, *Green Chem.*, 2016, **18**(15), 4145–4169.

41 W. Sriningsih, M. G. Saerodji, W. Trisunaryanti, R. Armunanto and I. I. Falah, *Proc. Environ. Sci.*, 2014, **20**, 215–224.

42 K. Kositkanawuth, M. L. Sattler and B. Dennis, *Curr. Sustainable/Renewable Energy Rep.*, 2014, **1**(4), 121–128.

43 R. Miandad, M. A. Barakat, M. Rehan, A. S. Aburiazaiza, I. M. I. Ismail and A. S. Nizami, *Waste Manage.*, 2017, **69**, 66.

44 J. S. Kim, W. Y. Lee, S. B. Lee, S. B. Kim and M. J. Choi, Degradation of polystyrene waste over base promoted Fe catalysts, *Catal. Today*, 2003, **87**, 59–68.

45 V. R. Chumbhale, J. S. Kim, W. Y. Lee, S. H. Song, S. B. Lee and M. J. Choi, *Eng. Chem.*, 2005, **11**, 253.

46 I. Elsayed and A. Eseyin, Production high yields of aromatic hydrocarbons through catalytic fast pyrolysis of torrefied wood and polystyrene, *Fuel*, 2016, **174**, 317–324.

47 K. Ding, S. Liua, Y. Huanga, S. Liub, N. Zhoub, P. Peng, Y. Wang, P. Chen and R. Ruan, *Energy Convers. Manage.*, 2019, **196**, 1316–1325.

48 A. Nzihou, B. Stanmore, N. Lyczko and D. P. Minh, *Energy*, 2019, **170**, 326–337.

49 A. Van Der Ent, D. L. Callahan, B. N. Noller, J. Mesjasz-Przybylowicz, W. J. Przybylowicz, A. Barnabas and H. H. Harris, *Sci. Rep.*, 2017, **7**, 41861.

50 M. Said, L. Cassayre, J. L. Dirion, A. Nzihou and X. Joulia, *Ind. Eng. Chem. Res.*, 2018, **57**, 9788–9797.

51 K. Mette, S. Kühl, A. Tarasov, M. G. Willinger, J. Kröhnert, S. Wrabetz, A. Trunschke, M. Scherzer, F. Girgsdies, H. Düdder and K. Kähler, *ACS Catal.*, 2016, **6**, 7238–7248.

52 B. H. Lipshutz, *Adv. Synth. Catal.*, 2001, **343**(4), 313–326.

53 A. Roustila, C. Severac, J. Chêne and A. Percheron-Guégan, *Surf. Sci.*, 1994, **311**, 33–44.

54 K. Hearon, L. D. Nash, J. N. Rodriguez, A. T. Lonnecker, J. E. Raymond, T. S. Wilson, K. L. Wooley and D. J. Maitland, *Adv. Mater.*, 2014, **26**, 1552–1558.

55 R. S. Chauhan, S. Gopinath, P. Razdan, C. Delattre, G. S. Nirmala and R. Natarajan, *Waste Manage.*, 2008, **28**, 2140.

56 F. Abnisa, W. W. Daud and J. N. Sahu, *Environ. Prog. Sustainable Energy*, 2014, **33**, 1026–1033.

57 P. Rutkowski and A. Kubacki, *Energy Convers. Manage.*, 2006, **47**, 716–731.

58 M. Rehan, R. Miandad, M. A. Barakat, I. M. I. Ismail, T. Almeelbi, J. Gardy and A. S. Nizami, *Int. Biodeterior. Biodegrad.*, 2017, **119**, 162–175.

59 A. D. Russell, E. I. Antreou, S. S. Lam, C. Ludlo and H. A. Chase, *RSC Adv.*, 2012, **2**, 6756–6760.

60 P. Rex, I. P. Masilamani and L. R. Miranda, *J. Energy Inst.*, 2020, 1819–1832.

61 L. C. Lerici, M. S. Renzini and L. B. Pierella, *Procedia Mater. Sci.*, 2015, **8**, 297.

62 B. B. Uzoejinwa, X. He, S. Wang, A. E. F. Abomohra, Y. Hu and Q. Wang, *Energy Convers. Manage.*, 2018, **163**, 468–492.

63 S. Budsaereechai, A. J. Hunt and Y. Ngernyen, *RSC Adv.*, 2019, **9**, 5844.

64 K. Ding, S. Liua, Y. Huanga, S. Liub, N. Zhoub, P. Peng, Y. Wang, P. Chen and R. Ruan, *Energy Convers. Manage.*, 2019, **196**, 1316–1325.